

Universal anti-baryon density in e^+e^- , γp , pp , pA and AA collisions

Haidong Liu^{a,b,c}, Zhangbu Xu^b

^a*University of Science & Technology of China, Anhui 230027, China*

^b*Brookhaven National Laboratory, Upton, New York 11973*

^c*Lawrence Berkeley National Laboratory, Berkeley, California 94720*

Abstract

We compiled the systematical measurements of anti-nucleus production in ultra-relativistic heavy ion collisions as well as those in pp , $p\bar{p}$, γp and e^+e^- at various beam energies. The anti-baryon phase space density inferred from \bar{d}/\bar{p} ratio in $A+A$, $p+A$, $pp(\bar{p})$ and γp collisions is found to follow a universal distribution as a function of center of mass of beam energy and can be described in a statistical model. We demonstrated that anti-baryon density in all the collisions is the highest when the collisions are dominated by the processes of $g+g$ or $\bar{q}+g$. In e^+e^- collisions at LEP, the cross section of $q\bar{q}g$ is suppressed by a factor of strong coupling constant α_s relative to $q\bar{q}$. This can consistently explain the \bar{d} suppression observed by ALEPH relative to that in $e^+e^- \rightarrow ggg$ by ARGUS. We discuss the implications to the baryon enhancement at high transverse momentum at RHIC when jet is quenched.

Key words: anti-baryon production, phase space density, thermal properties

1 Introduction

Relativistic heavy ion collisions create high energy density and high baryon density in the reaction zone. Light nuclei and their antiparticles can be produced by the recombination of created nucleons and anti-nucleons or stopped nucleons [1,2,3,4]. This recombination process is called coalescence. Since the binding energy of nucleus is small, coalescence can only happen at the late stage of the evolution when the interactions between nucleons and other particles such as pions are weak. Therefore, the production of nucleus provides a tool to measure baryon distribution at the thermal freeze-out where the interactions between particles are weakening. Since the probability of coalescence of a particular nuclear system (d, 3He , etc.) depends on the properties of the

hadronic system formed at late stage as a result of the collision, its evolution and hadronization, the study of the coalescence process is useful in elucidating those properties. For example, in a coalescence model, the coalescence probability depends on the temperature, baryon chemical potential (essentially the baryon density), and the size of the system, as well as the statistical weight (degeneracy) of the coalesced nucleus [5]. From the measurement of the nucleus production, we will be able to construct the thermal freeze-out in the (T, μ_B) phase diagram [2]. Together with the measurements of other particle yields from which the statistical model can construct the chemical freeze-out, we will be able to have a better understanding of how the system evolves from chemical to thermal freeze-out.

How baryons are created and interact among themselves and with other particles in the course of the evolution of the system is an important subject in relativistic heavy ion collisions. The coalescence process is not unique in relativistic heavy ion collisions. In fact, the idea was originated from elementary particle collisions where it was used to formulate nucleus production [6]. Systematically measuring the coalescence effect of nucleons in collisions such as e^+e^- , pp , $\bar{p}p$, pA and AA may give us insight in this subject. Analytic formulae from coalescence models [1,2,3,7,4] can be used to extract the information. Transport models [1,4] with detailed phase space distribution of nucleons at coalescence have been used as well.

The formula of coalescence is of the form:

$$E_A \frac{d^3 N_A}{d^3 p_A} = B_A (E_p \frac{d^3 N_p}{d^3 p_p})^Z (E_n \frac{d^3 N_n}{d^3 p_n})^{A-Z} \quad (1)$$

where $E \frac{d^3 N}{d^3 p}$ is the invariant yield of nucleons or nuclei, A is the nuclear number of the produced nucleus and N, Z are the numbers of neutron and proton in the nucleus respectively. the differential cross section of the anti-deuteron is denoted as \bar{d} and that of the anti-proton as \bar{p} for simplicity in some cases in the following discussions. Simple coalescence, density matrix, sudden approximation and thermodynamic models predict a slightly different expression of B_A [1]. The fragment coalescence model[3] can be used to extract the source radii for different nuclei at their 'freeze-out' from its yields and the yields of smaller fragments. If assuming Gaussian sources, for the case of A=2 (deuteron) from nucleon coalescence (ignoring isospin difference):

$$\frac{d^3 N_d}{d^3 p_d} = \frac{\pi^{3/2} \frac{d^3 N_n}{d^3 p_n} \frac{d^3 N_p}{d^3 p_p}}{(R_G^2 + \rho_d^2/2)^{3/2}} \exp(\Delta E/T) \quad (2)$$

where ρ_d is the size parameter of the composite's wave function [3], $p + n \rightarrow d + \Delta E$, ΔE is the excess of binding energy for that channel. This source radius

(R_G) should be comparable to the source size from two-particle interferometry (HBT). In collisions with small reaction volume such as in pp and pA, the size of the nucleus and a maximal relative momentum (p_0) between the coalescing nucleons dominate ($\rho_d \gg R_G$). This results in an approximate constancy of B_A parameter characterized as momentum space coalescence volume, independent of beam energies and beam species. On the other hand, the phase space density is $[4/3/(2\pi)^2]\bar{d}/\bar{p}$ regardless of the system [7]. Recent development began to focus on the phase space aspects of the coalescence process which also tried to take into account the dynamical expansion. For the coalescence with nucleons and nuclei of low transverse momentum and middle rapidity, Eq.2.14b in Ref. [2] can be further simplified as:

$$\frac{d^2 N_A}{2\pi p_T dp_T dy} \simeq \frac{2J_A + 1}{(2\pi)^3} e^{(\frac{\mu_A - M}{T})} M_T V_{eff} e^{(-\frac{M_T - M}{T^*})} \quad (3)$$

The ratio of the differential cross sections of anti-deuteron (denoted as \bar{d}) to anti-proton (denoted as \bar{p}) is therefore related to the phase space density of the nucleon [7], the baryon chemical potential and thermal freeze-out temperature in coalescence model. In this paper, we will mainly discuss the experimental results in terms of phase space density, baryon chemical potential and thermal freeze-out temperature from coalescence measurements. Most of the discussion and calculation are related to Eq. 3. The quantity of $\frac{2J_A + 1}{(2\pi)^3} M_T V_{eff} e^{(-\frac{M_T - M}{T^*})}$ depends on details of the dynamics of the system, quantum effect, binding energy of nucleus and the selected p_T range. This is taken as a constant (C) for coalescence at low p_T for a given colliding system

$$\frac{d^2 N_A}{2\pi p_T dp_T dy} \simeq C e^{(-\frac{(m_B \pm \mu_B)A}{T})} \quad (4)$$

2 Chemical and Thermal Properties of Anti-nucleus Production

Production of light nuclei in heavy ion collisions has been measured by many groups at different beam energies and colliding systems[8] from BELAVAC to RHIC energies. A reasonable list of the measurements can be found in [8]. The results discussed here are results from E864 at the AGS [9,5,10], NA52 at SPS [11] and STAR at RHIC [12]. Fig. 1 shows the invariant yields of 18 hadrons being measured in a selected rapidity (y) and transverse momentum (p_T) bin by E864. It has been observed that a striking exponential dependence of light nuclei production up to $A = 7$ over ten orders of magnitudes in the invariant yield including nuclei and anti-nuclei [5,9,10]. Invariant yields are calculated and presented in terms of $d^2 N / (2\pi p_T dp_T dy)$ in units of $GeV^{-2} c^2$ per central collision. E864 Collaboration has fitted the production of the ten stable

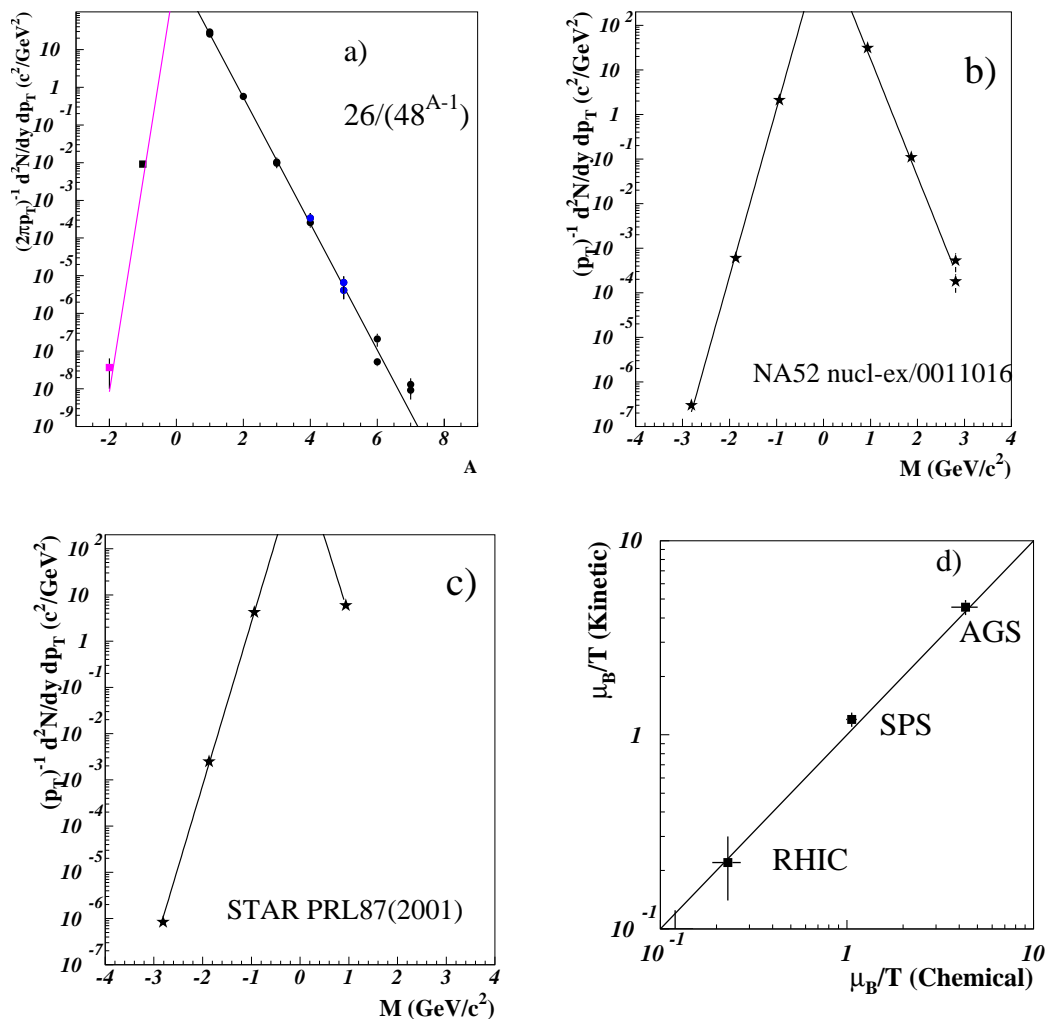


Fig. 1. a) Eighteen hadrons measured by E864 [9]. Stable light nuclei[13] are selected from $y = 1.9$ and $p_T/A < 300 \text{ MeV}/c$. \bar{p} is at $y = 1.9$ and $p_T \simeq 0$ [14]. \bar{d} is at $y = 1.9$ and $0 < p_T < 1 \text{ GeV}/c$. Lines are fits to the data assuming local thermal equilibrium. See text for details. Similar measurements are from NA52/SPS [11] and STAR/RHIC [12] and PHENIX/RHIC at higher p_T [17] as presented in b) and c), respectively. d) The measured μ_B/T at thermal freeze-out vs that at chemical freeze-out.

light nuclei with an exponential as a function of nuclear (baryon) number. The best fit[13] is $26/48^{A-1}$.

The difference between fugacity of proton λ and neutron λ' comes from the difference of the isospin abundance or n/p ratio in a thermal distribution. From neutron measurement[18] of $n/p = 1.19 \pm 0.08$, we have $\lambda' = 1.1\lambda$. For simplicity, the average fugacity or chemical potential are taken as: $\lambda_B = \sqrt{\lambda\lambda'}$, and $\mu_B = (\mu_p + \mu_n)/2$. Due to secondary nucleus production from beam pipe and limited p_T range of PID from dE/dx [12], STAR is only able to identify and measure light anti-nuclei (\bar{d} , ${}^3\bar{H}e$), \bar{p} and proton. Fig. 1 (right panel) shows

the measured differential yield at $p_T/A \simeq 0.4$ GeV/ c as function of particle's atomic number A for $p, \bar{p}, \bar{d}, \overline{{}^3\text{He}}$.

Using Eq. 4, we are able to fit well the nucleus production at low p_T at AGS, SPS and RHIC heavy ion collisions and obtain temperature and baryon chemical potential at kinetic freeze-out. The different slopes of baryons and antibaryons allow the determination of μ_B . The results are: $T = 126\text{MeV}$, $\mu_B = 21\text{MeV}$ (RHIC); $T = 130\text{MeV}$, $\mu_B = 170\text{MeV}$ (SPS); $T = 110\text{MeV}$, $\mu_B = 500\text{MeV}$ (AGS). Errors were estimated to be $\pm 10\text{MeV}$ for all the cases [13]. Fig. 1.d shows the ratios of μ_B/T at kinetic freeze-out vs that at chemical freeze-out at AGS, SPS and RHIC central AA collisions. The measurements are indeed consistent with each other even though the parameters at chemical freeze-out are extracted from thermal fit to the many ratios of the integrated particle yields [16] while the parameters from coalescence are from nuclear cluster formation rate at low p_T . However, whether such a trajectory along the phase diagram is possible requires further study since some of the studies [19] suggest a path of constant ratio of entropy to baryon number where as temperature drops baryon chemical potential increases. The coalescence measurement suggests a path corresponding to large entropy increase from chemical to thermal freeze-out.

3 Anti-baryon Density

The coalescence measurement is also sensitive to the phase space of baryon and anti-baryon [7]. For example, \bar{d}/\bar{p} (ratio of the differential cross sections) can be taken as a measure of the anti-baryon phase space density at kinetic freeze-out where coalescence happens. Data of \bar{d}/\bar{p} ratio from various beam energies and colliding species ($pp, \bar{p}p, pA, AA$) [21,22,23,24,25,5,9,11,15,12,17] were collected and shown in Fig. 2. One very interesting observation is that the ratio increases monotonically with beam energies and reaches a plateau above ISR beam energy regardless of the beam species (pp, pA, AA). Similar behavior has been seen in \bar{p}/p ratio as a function of beam energy [20]. This similar trend is quite nature in terms of thermal model and coalescence as shown in Eq. 3. The relation between \bar{d}/\bar{p} and \bar{p}/p is

$$\bar{d}/\bar{p} \simeq \exp(-m_B/T) \times \sqrt{\bar{p}/p}$$

where m_B is the nucleon mass and T is the freeze-out temperature. The curves in Fig. 2 correspond to three choices of $T = 130, 120, 110$ MeV. This relation shows qualitative agreement with a fixed freeze-out temperature at about 120MeV. Recently, CERES Collaboration observed a universal thermal freeze-out behavior [26]. These two measurements may be closely related. However, It also indicates that the temperature may slightly depend on beam energy with

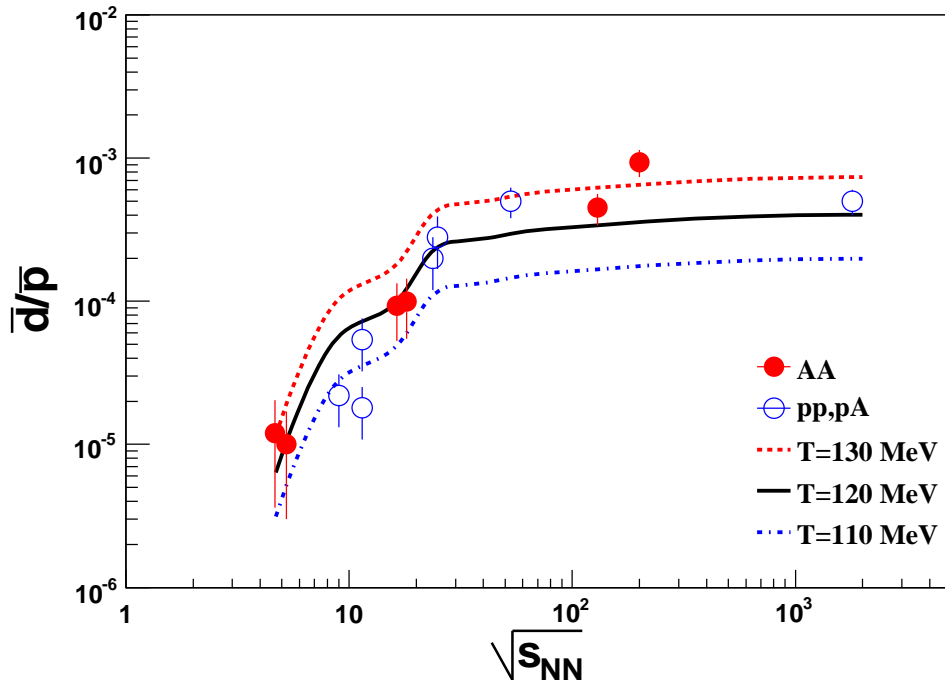


Fig. 2. \bar{d}/\bar{p} as a measure of antibaryon phase space density as a function of beam energy for pp, pA and AA collisions. The curves are $\exp(-m_B/T) \times \sqrt{\bar{p}/p}$ for three choices of T at 130MeV, 120MeV and 110MeV.

lower temperature at lower \sqrt{s} and higher value at higher \sqrt{s} . These findings suggest that the anti-nucleons are produced and coalesce in a statistical fashion in $A+A$, $p+A$, $p+p$ and γp collisions at similar density. Final state interactions in nucleus-nucleus collisions do not change this aspect. It also shows that correlations among anti-nucleons in momentum and coordinate space do not alter the \bar{d} yields since its production can be described statistically.

4 Microscopic Processes Creating Anti-deuterons

We tabulate the collision system, their dominant processes and \bar{d}/\bar{p} in Tab. 1. Table 1 and Fig. 3 show that collisions dominated by $\bar{q}+g$ and/or $g+g$ saturate anti-baryon density at 10^{-3} while those dominated by $q+q(\bar{q})$ or $q+g$ produce much less anti-baryons [27,28,29]. It is very convincing from the collisions in γp and e^+e^- at various energies. The measurements at e^+e^- and γp may be used to gauge what kind of partonic configuration creates baryons. There are two measurements of \bar{d}/\bar{p} from e^+e^- at low energies [27]: one at Υ mass of $\sqrt{s} = 9.86$ where the final state hadrons are predominantly from Υ decay to three gluons (ggg) and the other an upper limit at continuous energy of $\sqrt{s} = 10.GeV$ where the final state hadrons come from $q\bar{q}$ pair from a virtual photon. These two ratios are different by more than a factor of 3. This may

| system | processes | \bar{d}/\bar{p} |
|---------------------|----------------|--------------------------------|
| $e^+e^- (\Upsilon)$ | ggg | $7.4_{-2.0}^{+3.6} 10^{-4}$ |
| $\gamma p(200)$ | $q\bar{q}g$ | $5.0 \pm 1.1 \times 10^{-4}$ |
| $pp(53)$ | $qg, \bar{q}g$ | $5.0 \pm 1.2 \times 10^{-4}$ |
| $p\bar{p}(1800)$ | $qg, \bar{q}g$ | 5.0×10^{-4} |
| $AA(130)$ | $qg, \bar{q}g$ | $4.5 \pm 1.1 \times 10^{-4}$ |
| $e^+e^- (10)$ | $q\bar{q}$ | $< 2.1 \times 10^{-4}$ |
| $e^+e^- (91)$ | $q\bar{q}$ | $(8.4 \pm 2.7) \times 10^{-5}$ |
| $pp(A)(< 20)$ | qg, qq | $< 10^{-4}$ |
| $AA(< 20)$ | qg, qq | $10^{-4} - 10^{-5}$ |

Table 1

Dominant processes in different collision systems and the corresponding \bar{d}/\bar{p} ratio. Values in the parentheses are the center of mass beam energy in GeV.

be related to how baryons are created (more baryon from gluons than from quarks). In fact, not only the \bar{d}/\bar{p} are different in these two e^+e^- collisions, the baryon production is higher at Υ than at the continuous energy while the meson production is the same. The anti-baryon phase space density from ggg configuration in e^+e^- is very similar to the anti-baryon phase space density measured at RHIC. The \bar{d}/\bar{p} ratio from the $\bar{q}q$ configuration is much lower. On the other hand, γp collisions [28], where the dominant process is $q\bar{q} + g$, yield similar anti-baryon density as those in nucleus-nucleus collisions.

In addition, ALEPH Collaboration [29] found that baryon production is suppressed in e^+e^- to hadron event relative to other system as shown in Fig. 3. The double ratio of \bar{d}/\bar{p} in e^+e^- between Z boson hadron decay events ($\bar{d}/\bar{p} = 8.4 \pm 2.7 \times 10^{-5}$) and $\Upsilon \rightarrow ggg$ events ($\bar{d}/\bar{p} = 7.4_{-2.0}^{+3.6} \times 10^{-4}$) is $\gamma_B = 0.11_{-0.06}^{+0.05}$. In those Z boson hadron events, the dominant process is $q\bar{q}$ fragmentation. However, the event rate of process $q\bar{q}g$, whose fragmentation would yield same \bar{d}/\bar{p} as in ggg , is suppressed by a factor of strong coupling constant $\alpha_s(M_Z) = 0.116$. We have shown in Table 1 and Fig. 3 that production of anti-deuterons is negligible in $q\bar{q}$ compared to $q\bar{q}g$ events, and both ggg (Υ) and $q\bar{q}g$ (γp) saturate \bar{d}/\bar{p} . The suppression of \bar{d}/\bar{p} by a factor of $\gamma_B = 0.11$ in e^+e^- at LEP can be readily explained by the event rate $e^+e^- \rightarrow q\bar{q}g$ at $\alpha_s(M_Z) = 0.116$. This observation can be further tested by measuring \bar{d}/\bar{p} in $e^+e^- \rightarrow \bar{q}q$ and $e^+e^- \rightarrow \bar{q}qg$ separately at LEP or other facilities. The baryon production in a gluon jet is indeed about a factor of 2 higher than that in a quark jet as measured separately at LEP. This will not explain a factor of 10 differences in baryon phase space density. On the other hand, the particle spectra in a gluon jet are in general softer than those in a quark jet. This condensation in momentum and coordinate spaces increases the phase space

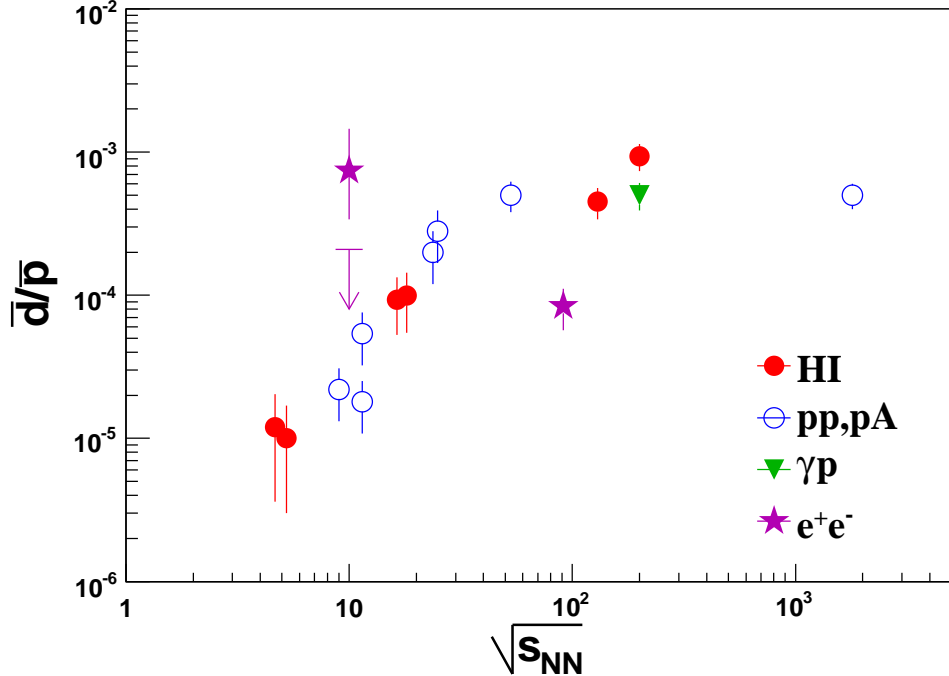


Fig. 3. \bar{d}/\bar{p} as a measure of antibaryon phase space density as a function of beam energy for various beam species. e^+e^- and γp collisions are also shown at their center of mass beam energy.

density of the baryons. From Table 1, it is inconclusive whether $q + g$ produces less anti-baryons at low beam energy due to low production of anti-deuteron in this configuration or due to energy threshold in producing anti-deuterons. In any case, it is conclusive that baryon density from collisions involving a gluon is much higher than those without gluon.

5 Implications to Baryon/Meson Enhancement and Jet Quenching at RHIC

Although what presented here are measurements of anti-deuteron production at relatively low p_T , it requires a total energy of at least $W = 3.8$ GeV in an elementary collision. This is not a soft process even though coalescence is a final state interaction. In what follows, we attempt to apply the observation that baryons (anti-baryons) are produced by processes of $q + g$ and $g + g$ ($\bar{q} + g$ and $g + g$) to the baryon enhancement at high p_T at RHIC when jet is quenched in the strongly interacting QCD matter.

At RHIC, baryons are enhanced relative to mesons toward more central Au+Au collisions at intermediate p_T [30,31,32] while elliptic flow is found to follow number of constituent quark scaling in the same p_T range [32]. Coalescence of quarks at hadronization can quantitatively explain these phenomena. At

higher p_T , baryons are expected to be more suppressed than mesons since gluons, which fragment relatively more to baryons than mesons, are more suppressed than quarks due to a casimir color factor of 9/4 in parton energy loss when they traverse hot and dense QCD medium. Experimentally, the suppressions of baryons and mesons at high p_T are observed to be the same by STAR at RHIC [33]. Compton-like scattering with leading quark and gluon conversions in the quark-gluon plasma can explain the phenomenon when large scattering cross section is assumed [34]. On the other hand, if $q + g$ configuration can always enhance baryon production regardless of whether gluon or quark is leading parton, the required large parton cross section can be compromised.

6 Conclusions

In summary, we presented systematically the anti-baryon density inferred from \bar{d}/\bar{p} measurements in various collision systems at various energies. It was found that the density in γp , pp, pA and AA collisions follows a universal distribution as function of beam energy and can be described statistically. The anti-baryon density at the coalescence saturates when the processes from different collisions involving gluons. The suppression of baryon density at LEP is due to low event rate involving gluon jets. We stipulated a possible explanation of large \bar{p}/π ratio in the intermediate p_T and high p_T at RHIC.

7 Acknowledgements

The authors thank Drs. J.M. Engelage, E. Finch, N. George, D. Hardtke, C.M. Ko, R. Majka, R. Rapp, F.Q. Wang and N. Xu for valuable discussions. This work was supported in part by the HENP Divisions of the Office of Science of the U.S. DOE; the Ministry of Education and the NNSFC of China. XZB was supported in part by a DOE Early Career Award and the Presidential Early Career Award for Scientists and Engineers.

References

- [1] J.L. Nagle *et al.*, Phys. Rev. C **53**, 367 (1996).
- [2] R. Scheibl, U. Heinz, Phys. Rev. C **59**, 1585 (1999).
- [3] W.J. Llope *et al.*, Phys. Rev. C **52**, 2004 (1995).

- [4] R. Bond *et al.*, Phys. Lett. B **71**, 43 (1977); A. Baltz *et al.*, Phys. Lett. B **325**, 7 (1994); R. Mattiello *et al.*, Phys. Rev. C **55**, 1443 (1997); P. Braun-Munzinger *et al.*, Phys. Lett. B **334**, 43 (1995); A.Z. Mekjian, Phys. Rev. C **17**, 1051 (1978); H. Sato and K. Yazaki, Phys. Lett. B **98**, 153 (1981); J.I. Kapusta, Phys. Rev. C **21**, 1301 (1980).
- [5] T.A. Armstrong *et al.*, Phys. Rev. C **61**, 064908 (2000); T.A. Armstrong *et al.*, Phys. Rev. Lett. **83**, 5431 (1999); T.A. Armstrong *et al.*, Phys. Rev. Lett. **85**, 2685 (2000).
- [6] A. Schwarzschild *et al.*, Phys. Rep. **129**, 854 (1963).
- [7] F.Q. Wang and N. Xu, Phys. Rev. C **61**, 021904 (2000); F.Q. Wang, Phys. Lett. B **489**, 273 (2000); P.J. Siemens and J.I. Kapusta, Phys. Rev. Lett. **43**, 1486 (1979); **43**, 1690(E) (1979); L.P. Csernai and J.I. Kapusta, Phys. Rep. **131**, 223 (1986).
- [8] N. George, Ph.D Thesis, Yale University, 1999.
- [9] T.A. Armstrong *et al.*, Phys. Rev. Lett. **85**, 2685 (2000).
- [10] T.A. Armstrong *et al.*, Phys. Rev. C **65**, 014906 (2002); T.A. Armstrong *et al.*, Phys. Rev. C **70**, 024902 (2004).
- [11] G. Ambrosini *et al.*, New J. Phys. **1**, 22.1 (1999); Heavy Ion Phys. **14** 297 (2001), e-print arxiv: nucl-ex/0011016.
- [12] C. Adler *et al.*, Phys. Rev. Lett. **87**, 262301 (2001).
- [13] Z. Xu *et al.*, e-print Arxiv: nucl-ex/9909012; nucl-ex/0207019.
- [14] T.A. Armstrong *et al.*, Phys. Rev. Lett. **79**, 3351 (1997); C. Adler *et al.*, Phys. Rev. Lett. **87**, 262302 (2001).
- [15] I.G. Bearden *et al.*, Phys. Rev. Lett. **85**, 2681 (2000).
- [16] N. Xu and M. Kaneta, Nucl. Phys. A **698**, 306c (2002); P. Braun-Munzinger *et al.*, Phys. Lett. B **365**, 1 (1996); P. Braun-Munzinger *et al.*, Phys. Lett. B **344**, 43 (1995).
- [17] S.S. Adler *et al.*, Phys. Rev. Lett. **94**, 122302 (2005).
- [18] T.A. Armstrong *et al.*, Phys. Rev. C **60**, 064903 (1999).
- [19] R. Rapp, Phys. Rev. C **66**, 017901 (2002); e-print Arxiv: hep-ph/0204131.
- [20] C. Adler *et al.*, Phys. Rev. Lett. **86**, 4778 (2001); L. Ahle *et al.*, Phys. Rev. Lett. **81**, 2650 (1998); F. Sickler *et al.*, Nucl. Phys. A **661**, 45c (1999); G. E. Copper, Ph.D Thesis, University of California at Berkeley, 2000; A.M. Rossi *et al.*, Nucl. Phys. B **84**, 269 (1975); M. Aguilar-Benitez *et al.*, Z. Phys. C **50**, 405 (1991).
- [21] F. Binon *et al.*, Phys. Lett. B **30**, 510 (1969).
- [22] J.A. Appel *et al.*, Phys. Rev. Lett. **32**, 428 (1974).

- [23] B. Alper *et al.*, Phys. Lett. B **46**, 265 (1973).
- [24] T. Alexopoulos *et al.*, Phys. Rev. D **62**, 072004 (2000).
- [25] M. Aoki *et al.*, Phys. Rev. Lett. **69**, 2345 (1992).
- [26] CERES Collaboration: D. Adamova *et al.*, Phys. Rev. Lett. **90**, 022301 (2003); nucl-ex/0207008.
- [27] H. Albrecht *et al.*, Phys. Lett. B **236**, 102 (1990).
- [28] A. Aktas *et al.*, Eur. Phys. J. C **36**, 413 (2004).
- [29] S.Schael *et al.*, Phys. Lett. B **639**, 192 (2006), e-print Arxiv: hep-ex/0604023.
- [30] S.S. Adler *et al.*, Phys. Rev. C **69**, 034909 (2004); J. Adams *et al.*, e-print Arxiv: nucl-ex/0606014.
- [31] J. Adams *et al.*, Phys. Rev. C **71**, 064902 (2005); J. Adams *et al.*, Phys. Rev. C **66**, 061901R (2002); J. Adams *et al.*, Phys. Lett. B **612**, 181 (2005).
- [32] J. Adams *et al.*, Phys. Rev. Lett. **92**, 052302 (2004).
- [33] J. Adams *et al.*, e-print Arxiv: nucl-ex/0606003.
- [34] W. Liu, C.M. Ko and B.W. Zhang, e-print Arxiv: nucl-th/0607047.